ELSEVIER

NeuroImage

www.elsevier.com/locate/ynimg
NeuroImage 32 (2006) 1106–1112

# Sensory deficits and olfactory system injury detected by novel application of MEMRI in newborn rabbit after antenatal hypoxia–ischemia

Alexander Drobyshevsky,[a,*] Alan M. Robinson,[b] Matthew Derrick,[a] Alice M. Wyrwicz,[c] Xinhai Ji,[a] Ila Englof,[a] and Sidhartha Tan[a]

[a]*Department of Pediatrics, Evanston Northwestern Healthcare Research Institute and Northwestern University, 2650 Ridge Ave., Evanston, IL 60201, USA*
[b]*Dept. Otolaryngology-Head and Neck Surgery, Northwestern University, Evanston, IL, USA*
[c]*Center for Basic MR Research, Evanston Northwestern Healthcare and Northwestern University, Evanston, IL, USA*

Received 16 January 2006; revised 31 May 2006; accepted 2 June 2006
Available online 24 July 2006

**Sensory deficits are frequently observed in cerebral palsy patients. The motor response to smell was found to be abnormal in an animal model of cerebral palsy following fetal hypoxia–ischemia. We hypothesized that fetal hypoxia–ischemia causes long-lasting and selective olfactory tract injury. A population of newborn rabbits with motor deficits was selected after spontaneous delivery following uterine ischemia at 22 days gestation (E22, 70% term). $MnCl_2$, 20 mg/kg, was administered in both nostrils at postnatal day 1 (E32). One nostril was occluded to control for smell augmentation through the other open nostril by intermittent amyl acetate stimulation for 6 h. T1-weighted MRI images were obtained on newborn rabbits. Amyl acetate exposure increased augmentation of $Mn^{2+}$ uptake in olfactory epithelium on the open side in control group but the augmentation was decreased after hypoxia. The proportion of animals with a greater enhancement in the open side increased in controls after amyl acetate, but not in hypoxia. $Mn^{2+}$ took longer to arrive at the olfactory bulbs and the rate of subsequent increase was slower in hypoxia. Concomitantly, the thickness of olfactory epithelium and the number of mature olfactory neurons, detected on olfactory marker protein immunostaining, were significantly less in the hypoxic group. Functional MRI studies are superior to neurobehavioral smell testing in the rabbit kits as they are more sensitive and quantifiable measures and do not depend upon the motor response. Antenatal hypoxia–ischemia causes long-lasting injury to neuronal tracts of the olfactory system including olfactory epithelium.**
**© 2006 Elsevier Inc. All rights reserved.**

## Introduction

Sensory deficits are frequently observed in cerebral palsy (CP) patients (Van Heest et al., 1993) but there are very few studies of the sensory system that investigate hypoxia-induced injury. The recent development of an animal model of CP in rabbits has made it possible to investigate concomitant sensory deficits following fetal hypoxia–ischemia. Olfactory function is critically important for a newborn rabbit, which is born blind and deaf. With the sense of smell and touch newborn rabbits find their way to the mother's nipples for feeding. Smell deficits elicited by the aversive motor response to certain odorants were observed in the newborn rabbits manifesting the CP phenotype in our previous study of antenatal hypoxia–ischemia in rabbits (Derrick et al., 2004). Acute placental insufficiency is achieved by uterine ischemia resulting in global hypoxia–ischemia to the 70% gestation fetus and mimics the insult of abruptio placentae. The surviving rabbit kits manifest multiple motor and sensory deficits, including muscle hypertonia and postural deficits, impaired locomotion, deficits in righting, suck and swallow reflexes; in addition, deficits of smell and facial touch are observed (Derrick et al., 2004; Tan et al., 2005). The concomitant motor deficits could have affected the results of the olfactory testing. Therefore, we sought to quantitatively assess functional deficits in the olfactory system independent of the motor response in the affected rabbits.

Manganese-enhanced magnetic resonance imaging (MEMRI) is a non-invasive, quantitative tool to measure neuronal functional activity based on the ability of neurons to uptake manganese ion ($Mn^{2+}$) via calcium channels and actively transport it via axonal transport. $Mn^{2+}$ is a paramagnetic contrast agent that can cross synaptic barriers. MEMRI has been successfully applied for *in vivo* neuronal tract and functional region visualization (Pautler et al., 1998; Yu et al., 2005), neuronal plasticity (Van der Linden et al., 2004) and for the quantitative assessment of neuronal injury after trauma (Bilgen et al., 2005) or hypoxia–ischemia (Aoki et al., 2004).

* Corresponding author. Fax: +1 847 570 0231.
*E-mail address:* oldrobys@northwestern.edu (A. Drobyshevsky).
**Available online on ScienceDirect (www.sciencedirect.com).**

1053-8119/$ - see front matter © 2006 Elsevier Inc. All rights reserved.
doi:10.1016/j.neuroimage.2006.06.002

The olfactory system is particularly suited for investigation by MEMRI due to high neuronal activity, ease of application and ready uptake of the contrast (Pautler and Koretsky, 2002). We modified the neuronal tracing technique for the olfactory system (Pautler and Koretsky, 2002) to quantitatively assess the difference in $Mn^{2+}$ uptake and transport by olfactory epithelium neurons between control and post-hypoxic rabbit kits with motor deficits. We hypothesized that fetal global hypoxia–ischemia causes injury to the neurons in the olfactory epithelium and results in longstanding deficits that extend to the postnatal period. Herein, we show that fetal hypoxia–ischemia delays the appearance of $Mn^{2+}$ by 7% in the olfactory bulbs postnatally with odorant stimulation; in addition, the rate of accumulation (22%) and the absolute amount (14%) is also decreased. Concomitantly, there is greater olfactory epithelium injury by histopathology.

## Methods

### *Prenatal hypoxia–ischemia model*

*In vivo* global hypoxia–ischemia of fetuses was induced by sustained uterine ischemia at 22 days gestation (70% term) in timed pregnant New Zealand white rabbits (Myrtle's Rabbits, Thompson Station, Tennessee) as described previously (Derrick et al., 2004). This modeled acute placental insufficiency at a premature gestation. Briefly, dams were anesthetized and a balloon catheter introduced into the left femoral artery and advanced into the descending aorta to above the uterine and below the renal arteries. The balloon was inflated for 40 min. Then, the balloon was deflated and the catheter removed. The femoral artery was repaired and the skin occluded. The dam was allowed to deliver in a nest box at term (31.5 days). The time from episode of hypoxia–ischemia to MEMRI and behavioral testing was 10 days, almost one-third gestation.

### *Behavioral testing*

At postnatal day 1 (P1 = E32) kits underwent neurobehavioral testing for the presence of sensory and motor deficits, including the test for aversive reaction to amyl acetate as described previously (Derrick et al., 2004). Olfaction was tested by aversive response to a cotton swab soaked with odorant. The test was videotaped (see movie in the Supplementary materials) and the results were scored from 0 (no reaction) to 3 (active avoidance), assessed by 2 observers, who were blinded to the experimental groups. There was no direct skin or mucosal contact with the cotton swab (as shown in our video). A population of rabbits with postural and motor deficits (about 75% incidence) was chosen for MEMRI imaging.

### *Groups*

Controls: Naive P1 rabbit kits.
Hypoxia: P1 rabbit kits that were subjected to antenatal hypoxia–ischemia at E22.

### *MRI imaging*

All rabbit kits were sedated with intramuscular injection of ketamine (35 mg/kg), xylazine (5 mg/kg) and acepromazine (1.0 mg/kg) and imaged in 4.7T Bruker BioSpec scanner with a 28-mm birdcage coil. The animal rectal temperature was maintained at 37°C, in normal physiological range for P1 rabbit kits, by using heated water blanket. T1-weighted (TR/TE = 220/6 ms, NEX = 5), T2-weighted (TR/TE = 4000/50 ms, NEX = 5) and inversion recovery spin-echo sequence (TR/TE = 3500/9.7 ms, 9 inversion times from 10 to 2500 ms) images were acquired in the same slice position, 2 mm slice thickness, FOV 20 mm and 128 × 64 matrix. T1 parametric maps were calculated by 2-parameter non-linear fitting of inversion times verses pixel intensities, obtained with the inversion recovery sequence, using in-house software written in MATLAB 7.0.4 (The Mathworks Co, Natick, MA).

To ensure reproducible position of the imaging sections, 5 coronal slices, 2 mm thick, were placed perpendicular to the plane connecting the most inferior point of cerebrum, as determined with the aid of multi-slice sagittal localizer scan, and the center of the third slice was placed in the middle cross-section of olfactory bulbs. The first slice covered nasal turbinates with olfactory epithelium and the last slice a portion of piriform cortex. Regions of interest (ROI) were placed on the T2-weighted image for the donut-shaped glomerular layer of olfactory bulbs (OGL) and medial–dorsal portion of the prefrontal cortex. Intensities derived from T1 image were normalized by values from the medial prefrontal cortex ROI, where there was no enhancement by $Mn^{2+}$, or by ROI placed on the vitreous body in the rabbits' eye. Without $MnCl_2$ administration, no significant difference was observed in the ratio of intensities of olfactory bulb to cortex between hypoxic (95% confidence intervals 0.996–1.222) and control groups (0.937–1.174, $p = 0.65$, $t$ test). However, there was significant maturational change in T1 relaxation time in olfactory bulbs and cortex between P1 and P2 rabbits (see Results). Therefore, we preferred to normalize olfactory bulb intensities by cortex than by water phantom because the former normalization accounts not only for scanner gains, but also for maturational difference in T1 relaxation times.

### *Experiments*

Manganese chloride ($MnCl_2$) was obtained from Sigma (St. Louis, MO) and dissolved in saline. The solution was pipetted once into both nostrils, using a syringe with an attached plastic tube. Each nostril received 0.05 ml containing 10 mg/kg $MnCl_2$. The range in weights of the P1 rabbit kits was 45–65 g.

Four different experiments were conducted on separate sets of animals:

(1) To examine developmental changes in olfactory tissue, T1 parametric maps were obtained from 5 control rabbit kits at postnatal days 1 (P1), 2 and 5, without $MnCl_2$ application and odor stimulation.
(2) To study time course of $Mn^{2+}$ accumulation, a subset of control animals received 0.05 ml of water soluble electrolytic gel in one nostril, which temporarily blocked the nostril and prevented retropharyngeal transport of $MnCl_2$ that was administered immediately afterwards to the other nostril. The gel application caused an absence of MRI signal enhancement on that side in contrast to the signal enhancement on the $MnCl_2$ side. Unlike rodents, New Zealand rabbits do not have septal window, as evidenced from our MRI volumetric scans of the rabbit nasal cavity. The only communication between nostrils is retropharyngeal where septum detaches from palate. Three groups of kits ($n = 3$/group) were imaged after 6, 16 and 24 h of $MnCl_2$ adminis-

tration. Timing of $MnCl_2$ administration was adjusted so that all the 3 groups were imaged at the same time at P2. No odor stimulation was given.

(3) To study the rate of $Mn^{2+}$ propagation along olfactory axons, 4 control and 4 hypoxic kits were administered $MnCl_2$ in both nostrils. One of the nostrils was randomly closed with acrylic glue. An hour after the $MnCl_2$ administration, the animals were sedated, placed in the magnet and series of T1-weighted images were obtained for the next 4 h with 10 min temporal resolution. Odor stimulation was given in 15 min intervals by blowing air through a vaporizer (VixOne, Westamed, AZ) containing amyl acetate, diluted 1:10 in mineral oil, alternating with intervals of clear air. The time course of signal intensity change in olfactory bulbs was measured before and after odor stimulation. The time points with intensity of signal within 2 standard deviations of the initial average were considered as part of the baseline. The contrast accumulation rate was estimated as a slope of the regression line for the points exceeding the baseline. The intersection with the baseline was taken as the $Mn^{2+}$ arrival time. $Mn^{2+}$ propagation velocity was measured by the difference of $Mn^{2+}$ arrival time in two consecutive slices in olfactory bulbs, divided by the slice thickness.

(4) To examine the difference in $MnCl_2$ uptake in control and hypoxia groups, P1 rabbit kits were administered $MnCl_2$ in both nostrils. One of the nostrils was randomly closed with acrylic glue. A subset of animals (12 controls and 9 hypoxic kits) was given odor stimulation for 6 h, as in experiment 3. Another subset of animals (9 controls and 5 hypoxic kits) was given no stimulation. All rabbit kits underwent MRI examination 6 h afterwards.

*Histology and immunochemistry*

Immediately after MRI, a subset of rabbits (3 controls and 3 hypoxic kits) was euthanatized by anesthetic overdose. Rabbit heads were decalcified in 4% formic acid, 2% sodium citrate for two days at 4°C and dehydrated in graded ethanols (30%, 50%, 70%, 95% and 100%) followed by three changes of xylene and infiltrated over a two-hour period with three changes of molten paraffin wax under vacuum and embedded. Coronal rabbit head sections were cut at 7 μm and adhered to glass slides. Tissue sections were de-paraffinized with three changes of xylene and rehydrated to phosphate-buffered saline (PBS), pH 7.4, through graded ethanols.

The immunodetection protocol followed was essentially as supplied with the Vectastain ABC elite kit (Vector laboratories Inc., Burlingame, CA). In brief, tissue sections were blocked in 5% horse serum for 30 min then incubated for one hour at room temperature with goat anti-olfactory marker protein antiserum (goat anti-OMP from Frank L. Margolis, PhD, University of Maryland, Baltimore, MD) diluted 1:3000 in 5% horse serum in PBS. In brief, sections were washed in PBS and incubated for 30 min with biotinylated horse anti-goat IgG in 1% goat serum in PBS. After a PBS wash, sections were then incubated 30 min with avidin–biotin peroxidase conjugate. After a final PBS wash, the peroxidase substrate 3-3′ diaminobenzamidine (DAB) was used to develop a brown precipitate over 3 min. Sections were washed and counterstained with hematoxylin. Sections were washed in water and dehydrated in graded ethanols followed by three changes of xylene and coverslips applied with Neo-Mount (Harelco, Gibbstown, NJ). Digital images were made of stained tissue sections using an Insight camera (Diagnostic Instruments, Inc., Sterling Heights, MI) attached to a Leica DMRB light microscope.

Epithelial thickness (from apical surface to basal lamina) and OMP-positive neuron counts were performed on captured images. Regional variations within the kit heads were corrected for by taking coronal sections from three well-separated specific regions within the head. Anatomical landmarks were used to select these head regions and serial sections were mounted on glass slides. Region I was the most posterior region with sections containing olfactory bulbs and septum (similar location to Fig. 1B). Region II was approximately 2 mm anterior to Region I and was defined by having a septum with no visible vomeronasal organ, two turbinates and two distinct air cavities on each side of the septum. Region III was the most anterior region (approximately 3 mm anterior to Region II) defined by having a septum with a visible vomeronasal organ, three turbinates and two distinct air cavities on each side of the septum.

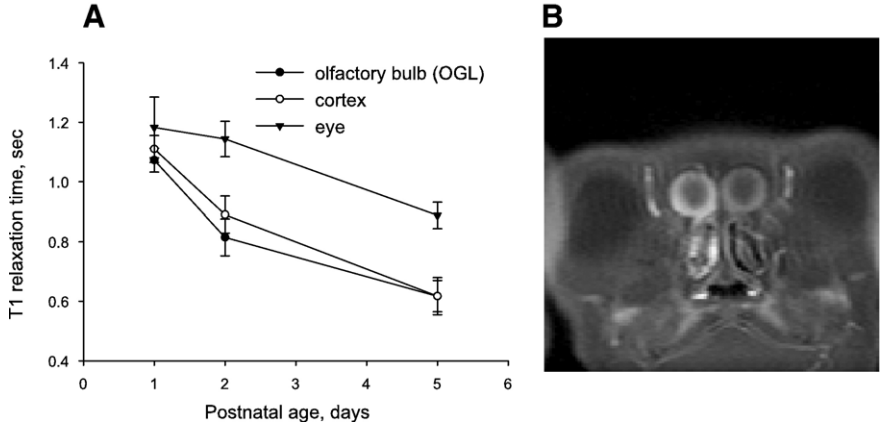


Fig. 1. (A) Decrease in T1 times in neonatal rabbit kits in brain tissue with maturation. The decrease of T1 time was significant across time from P1, P2 and P5 ($p<0.05$, ANOVA) in the olfactory bulb and cortex. The decrease of T1 in the eye was significant only between P2 and P5 ($p<0.05$, ANOVA with post hoc Tukey multiple comparison). (B) Enhancement of olfactory epithelium and olfactory bulbs was observed on the side of the $MnCl_2$ administration 6 h after $MnCl_2$ administration in one nostril (left side on the image).

Epithelial thickness measurements within these anatomical regions were made at similar locations from both sides of the head within the sections to further reduce variation. All regions demonstrated OMP expression as described. These regions were therefore olfactory epithelium and not respiratory. A total of four serial sections per head region with four location-matched high power fields per section were used for measurements (250 μm epithelial length). Separate means of each of the location-matched fields were calculated for each head region in each animal. The average was therefore generated from measurements of a total 4 mm length of epithelium per region per animal.

Because epithelial thickness includes the uppermost (apical) layer of sustentacular (non-neuronal) cell bodies, thickness loss due to reduction in neuronal cells can be underestimated. Therefore, OMP-positive (mature) neurons were estimated by counting in similar captured images, except that three not four serial sections were evaluated. Counting was performed by hand tally counter and by marking off counted cell bodies on printed images. The criteria for positive neurons were that the cell body was immediately obvious (dark enough to be easily distinguished from background) and with a clearly defined border. Cell clumps, dark diffuse areas and faint staining was evaluated by microscopic examination of the original tissue sections because rabbit tissue has a higher background staining than rodent tissues with this antibody. These factors could be more easily evaluated on the original tissue sections.

### *Statistical analysis*

Data are presented as means ± SEM. Comparison across groups was done with *t* test, ANOVA or Wilcoxon signed rank test where appropriate. ANOVA with post hoc Tukey multiple comparisons was used in testing T1 relaxation times between animal ages. Differences with $p$ value less than 0.05 were considered significant. Correlation between ordinal neurobehavioral scores of smell with MEMRI was done with Spearman correlation coefficient ($r_s$).

## Results

### *Maturational changes in T1 relaxation times*

Application of MEMRI relies on changes in T1-weighted images and may be affected by normal maturational changes in T1 relaxation times. We found that T1 relaxation times of the rabbit brain rapidly decreased with development in the postnatal period (Fig. 1A) as has been reported previously for kittens (Baratti et al., 1999). The rate of decrease was more than 30% between P1 and P2, the period of investigation by MEMRI. The MEMRI values thus needed to be normalized to the intensity of an internal reference to account for confounding variables of the individual maturational changes in T1 relaxation time and different gain of the scanner amplifier. We investigated the cortex and eye for possible reference regions. T1 relaxation time in the cortex decreased at a similar rate to that in olfactory bulb (Fig. 1A), but in the eye, T1 relaxation times did not change much from P1 to P2 and only decreased by P5 when the rabbit kits opened their eyes. Because the cortex was found to be more suitable, all the signal intensities of the T1-weighted images were normalized by the intensities of the medial–dorsal portions of prefrontal cortex, where there was no evidence of $Mn^{2+}$ enhancement.

### *Enhancement in olfactory bulbs increased linearly during the first 24 h*

We applied $MnCl_2$ in one nostril of control rabbits and found that the intensity of the OGL in the olfactory bulbs on the side with $Mn^{2+}$ (Fig. 1B) increased linearly (regression, $r=0.93$) for the first 24 h and reached 57.4 ± 2.6% at a rate of 1.89 ± 1.6% per hour. This finding implied that MEMRI had to be measured at the same time for all groups in order to make a valid comparison. We chose the time point of 6 h as a compromise for the convenience of use, avoidance of unnecessary exposure of neonates and a reasonable increase (21.3 ± 2.2%) of signal, providing sufficient sensitivity to detect the differences in the contrast uptake between experimental groups.

### *Hypoxia–ischemia decreases postnatal $Mn^{2+}$ uptake with odorant*

We next compared $Mn^{2+}$ uptake in OGL with and without odorant stimulation in the control and hypoxic groups. There was no significant difference between hypoxia and control groups without odorant stimulation. $Mn^{2+}$ uptake was significantly decreased with the amyl acetate stimulation on the open (odorant exposed) side in hypoxic than control rabbits ($p<0.05$) (Fig. 2A).

### *Hypoxia–ischemia decreases the proportion of the animals with $Mn^{2+}$ uptake with odorant*

Normally, only 22% of the P1 rabbits (2 out of 9) showed greater $Mn^{2+}$ uptake on the open side than on the closed side. After odorant stimulation, this proportion increased to 64% in the controls (7 out of 12) (Fig. 2B). After fetal hypoxia, the proportion of P1 rabbits with greater $Mn^{2+}$ uptake on the open side (33%, 1 out of 3) did not show any difference from controls ($p>0.6$, Fisher's exact test). However, after odorant stimulation, the proportion with greater $Mn^{2+}$ uptake on the open side was lower in the hypoxia group (1 out of 9) than controls of kits ($p<0.03$, Fisher's exact test). Thus, not only was there a quantitative decrease in $Mn^{2+}$ uptake but the number of animals that differentially responded to odorant on the open side was also lower following fetal hypoxia.

### *Hypoxia–ischemia decreases the rate of $Mn^{2+}$ propagation with odorant stimulation*

To determine whether the difference in $MnCl_2$ enhancement in the olfactory bulbs between the control and hypoxic group was determined by a slower axonal transport or by reduced number of involved olfactory axons, we estimated the $Mn^{2+}$ arrival time and the slope of the enhancement curve. The time course of the dynamic signal change in OGL of olfactory bulbs was measured in a separate set of sedated rabbit kits (Fig. 3A). $Mn^{2+}$ contrast arrived later in hypoxia compared to controls in the open nostril side (Fig. 3B). Furthermore, the rate of increase of the signal in olfactory bulbs due to the $Mn^{2+}$ accumulation with time (i.e., contrast accumulation rate) was decreased in hypoxia compared to controls (Fig. 3C). Average $Mn^{2+}$ propagation velocity, measured by the $Mn^{2+}$ arrival time in two consecutive slices in olfactory bulbs, was 0.14 mm/min for controls and 0.11 mm/min for hypoxic kits.

### *Neurobehavioral testing did not correlate with $Mn^{2+}$ uptake*

The scores of the motor response to amyl acetate on neurobehavioral testing were markedly lower in the hypoxic

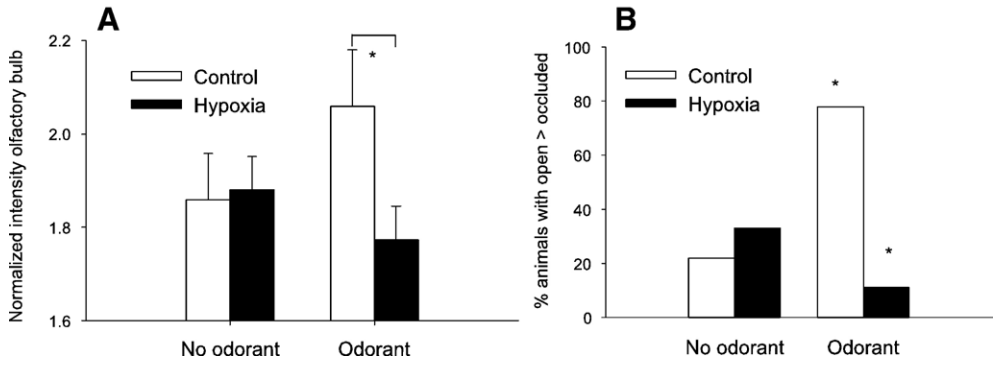


Fig. 2. (A) Normalized intensity in the olfactory bulbs on the open side in P1 kits following fetal hypoxia. The decrease relative to controls was significant when $Mn^{2+}$ uptake was augmented by amyl acetate stimulation (*$p<0.05$). (B) Proportion of animals with greater enhancement in open than in occluded side increased with odorant stimulation in controls. In contrast, hypoxia decreases this proportion (*$p<0.03$, Fisher's exact test). There was no significant difference in proportions without odorant stimulation.

group (1.32±0.95) compared to controls (3.0±0.0). The neurobehavioral test could not differentiate between different control P1 rabbits. There was little correlation between $Mn^{2+}$ enhancement in olfactory bulb with odor and neurobehavioral test of smell ($r_s=0.284$, $p=0.19$, $n=23$).

*Histopathological evidence of injury in olfactory epithelium*

Immunohistochemistry was performed to detect olfactory marker protein (OMP), a protein that is expressed by mature olfactory sensory neurons (Margolis, 1980). In the control rabbit kits, the OMP-positive neurons showed the typical regional pattern, delineating a band of mature neuron cell bodies within the pseudostratified olfactory neuroepithelium. This band of mature neurons is located between the neuron precursor cells (globose basal and flat basal cells on the apical surface of the lamina propria) and the sustentacular (supporting) cells that form a single layer of cells at the apical surface of the epithelium. This band is narrow, reflecting the relative immaturity of the newborn epithelium. However, there is a distinct difference between control epithelium and the hypoxic epithelium, in that the latter epithelium demonstrated patches of OMP-positive cells that appeared to be more randomly dispersed throughout the epithelium (Fig. 4). The overall appearance breaks up the typical pseudostratified layer of OMP-positive neuron cell bodies within the hypoxic rabbit kit epithelium.

The epithelial thickness in Region I, similar location illustrated in Fig. 1B (see Methods section for region descriptions), was significantly reduced in the hypoxic kits compared to control kits (44±2.1 vs. 55±2.9 μm, respectively) (*t* test, $p=0.01$). A similar finding occurred in Region II (43±2.2 vs. 54±2.6 μm, respectively) and Region III (43±2.1 vs. 55±2.5 μm, respectively).

The OMP-positive neuron count in Region I was significantly (*t* test, $p=0.01$) reduced in the hypoxic kits compared to control kits (34±8 vs. 130±11 neurons per 250 μm length of epithelium, respectively). A similar finding occurred in Region II (77±8 vs. 136±7 neurons, respectively) and Region III (77±6 vs. 112±6 neurons, respectively).

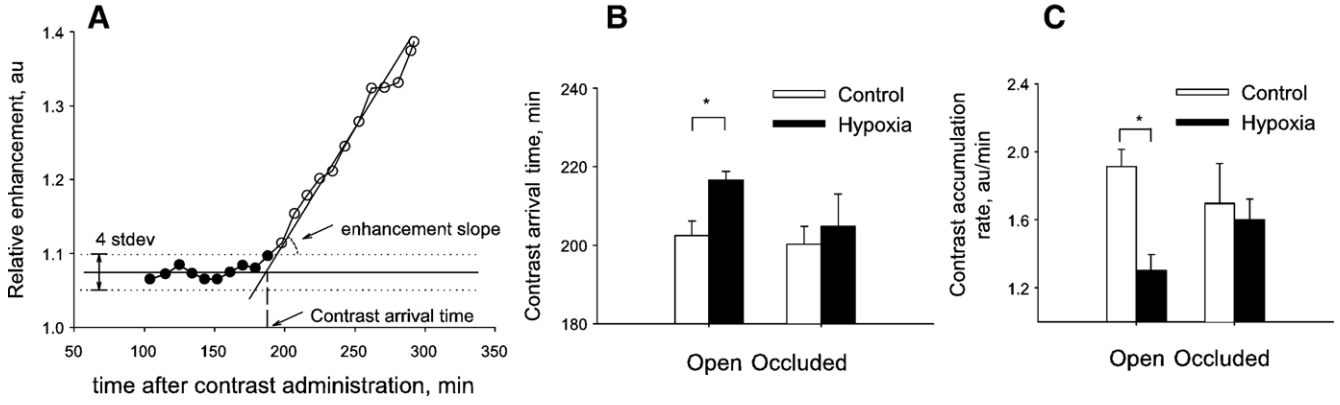


Fig. 3. (A) Time course of signal intensity change in olfactory bulbs, normalized to intensity in eye, were measured in sedated rabbit kits. Baseline included time points with intensity of signal within 2 standard deviations of the initial average. The contrast accumulation rate was estimated as a slope of the regression line for the points exceeding the baseline. The intersection with the baseline was taken as the $Mn^{2+}$ arrival time. (B) The $Mn^{2+}$ arrival time, estimated from the time course of olfactory bulbs intensity as in panel A, was significantly longer (B) and the accumulation rate was significantly smaller (C) in hypoxic group on the open side. *Significant difference in hypoxic group relative to controls ($p<0.05$, Wilcoxon signed rank test).

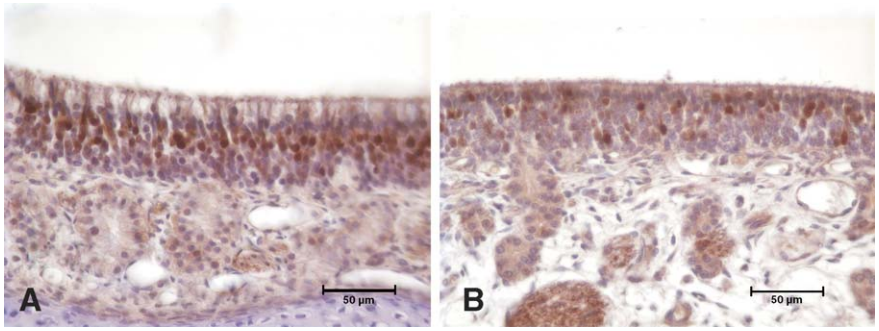


Fig. 4. Reduction in olfactory epithelium thickness and decrease in number of mature olfactory neurons in hypoxia group (B) relative to controls (A). Sections of olfactory epithelium were taken from midseptum nasal area and stained for olfactory marker protein (OMP). Scale bar 50 μm.

The reduction in epithelial thickness and reduction in OMP-positive neurons indicates fewer mature olfactory neurons are present in the hypoxic kit compared to the controls.

## Discussion

This study provides evidence for the first time, to the best of our knowledge, that fetal global hypoxia–ischemia causes long-lasting injury to the neurons of the olfactory epithelium in rabbit. Functional activity and axonal transport of olfactory neurons by MEMRI was affected in those newborn rabbits with motor deficits. There was delayed onset of $Mn^{2+}$ uptake, decreased rate of accumulation of $Mn^{2+}$ and decreased total amount of $Mn^{2+}$ uptake following fetal hypoxia–ischemia. This may be partly explained by the reduction in the quantity of mature olfactory neurons in the olfactory epithelium as determined by OMP staining, although it is possible that the surviving neurons were also injured and normal axonal transport was impaired. It is important to note that rabbit development is compressed compared to human development and the sensory deficits were discovered postnatally 10 days after the episode of fetal hypoxia–ischemia at 70% gestation. Thus, fetal H-I had long-lasting effects on olfactory deficits, lasting one-third rabbit gestation. These sensory deficits also occurred in a population selected for the motor deficits suggestive of cerebral palsy (Derrick et al., 2004) confirming human studies showing increased sensory deficits in CP patients (Van Heest et al., 1993).

Olfaction is very important to the newborn infant. The newborn's first attempt to locate the nipple and subsequent feeding behavior depends upon olfactory cues from the mother. Olfactory recognition is important for the mother–infant attachment process (Winberg and Porter, 1998). Other processes that olfaction is involved in are in the modulation of states of arousal or sleeping behavior; eliciting emotional behavior; providing directional cues to approach and withdrawal actions; anticipatory digestive physiology; and to contribute to the development of preferences in the alimentary and social domains (Schaal et al., 2004). The effect of H-I on olfaction in the perinatal period has not been well studied and this study aims to address this issue. Previous adult studies suggested that olfactory bulb and olfactory epithelium was relatively resistant to H-I-mediated damage (Nakashima et al., 1984; Hwang et al., 2003). However, recent studies have shown that this may not be the case in adults (Hwang et al., 2004) and olfactory deficits are observed in 10% stroke victims (Heckmann et al., 2005).

Because of the normal maturational decrease of T1 relaxation times during newborn development, we normalized the MEMRI values to the intensity of the medial prefrontal cortex that was not augmented by the contrast, instead of normalizing to a water phantom. The observed decrease in the contrast uptake in olfactory bulbs in the hypoxia group cannot be explained by the normalization procedure because the ratios of intensities of olfactory bulb to the regions used for normalization were not significantly different between the groups prior to $Mn^{2+}$ application.

This study made some important modification to the MEMRI methodology used previously (Pautler and Koretsky, 2002) for assessing *in vivo* olfactory function. By applying odor stimulation for longer time on awake animals, and sampling whole glomerular layer on a relatively thick slice, the method increased sensitivity and avoided bias in the selection of ROIs. Measurements of $Mn^{2+}$ arrival time and accumulation rate were done in sedated animals to control for motion, but the relative enhancement of the olfactory bulbs after 6 h of the $MnCl_2$ administration was on the whole less ($1.14 \pm 0.04$) than non-sedated animals ($1.86 \pm 0.07$).

Another modification made was occlusion of one nostril after $MnCl_2$ prior to odor stimulation. The occluded side was intended to serve as an internal control for $Mn^{2+}$ uptake. This led to unforeseen consequences of enhancement of $Mn^{2+}$ uptake in a majority of animals (but not all) on the occluded side. It is possible that control animals differ in their ability to handle simultaneous ambient odors and odor from the glue used to close the nostril. On the occluded side, the effect of any odor should be transient due to absence of airflow and habituation. On odorant stimulation via the open nostril, control rabbits enhanced $Mn^{2+}$ uptake ipsilaterally but hypoxic rabbits did not. It is unknown following fetal hypoxia–ischemia whether there was a loss of function or a delay in gain of function. Clearly, some baseline olfactory function was present even in hypoxic rabbits as there is similar $Mn^{2+}$ uptake to control animals without odor in both occluded and open sides.

Previous olfactory tests require animal training and depend on the motor response, exploratory response, mood and cooperation of the animal (Youngentob et al., 1997). It is our previous experience that the positive response to odorants depended heavily on the motor response and the subjective ordinal evaluation of this response. Because the motor response was principally affected in our model of CP, we have been concerned that the head responses in our neurobehavioral test for smell are not actually from olfactory deficits but reflect motor deficits, or could possibly be affected by

trigeminal nerve stimulation. Functional MEMRI has three important advantages over the previous olfactory tests. (1) It is an objective assessment independent of the motor capabilities of the animal. (2) It assesses one neuron *in vivo* – the olfactory neuron – and information is obtained to a single synapse. (3) It is quantitative in nature. MEMRI thus showed olfactory function when there was little or no response behaviorally to smell. At the same time, in our previous study, we did observe deficits in the neurobehavioral response even in those animals that had an intact motor response. Furthermore, the control animals had the same maximum neurobehavioral score but MEMRI showed some variability, suggesting that control rabbits may have different number of mature olfactory neurons and possible small differences in ability to smell could not be detected by the simple behavioral test.

The quantitative response could also serve as a valuable tool to investigate the repair response of the newborn rabbits to hypoxia–ischemia as the olfactory epithelium has a large cell turnover and abundance of stem cells (Schwob, 2002). Another big advantage of this MEMRI method was the ability to do repeated measurements non-invasively. Because olfactory neurons are easily accessible for manipulations, this model system is convenient to investigate different pathogenetic mechanisms following various perinatal insults.

There are many possible explanations to the depletion in olfactory neurons observed on histopathology. Fetal hypoxia–ischemia could have caused a direct injury to the olfactory epithelium. The other possibility is that the injury was at a more proximal level in the olfactory system. There is extensive feedback to the olfactory bulb from central structures and loss of this feedback may lead to apoptosis of sensory olfactory neurons in the epithelium (Farbman et al., 1988). Future avenues of research would be to investigate the influence of different odors not only on the dynamic amount of $Mn^{2+}$ uptake but to delineate different regions of enhancement in the olfactory bulb.

In summary, olfactory function can be assessed by axonal transport variables detected by MEMRI in the P1 rabbit kit. The fetal hypoxia–ischemic insult that results in motor deficits also results in long-lasting olfactory deficits discovered in the postnatal period. MEMRI provides a quantifiable tool superior to neurobehavioral testing based on the motor response.

## Acknowledgments

NIH NS 43285, NS41476, 1 S10 RR15685 We wish to thank Dr. Frank L. Margolis, University of Maryland, Baltimore, MD for providing OMP antibodies.

The study was supported by grants NIH NS 43285, NS41476, 1 S10 RR15685-01.

### Appendix A. Supplementary data

Supplementary data associated with this article can be found, in the online version, at doi:10.1016/j.neuroimage.2006.06.002.

## References

Aoki, I., Naruse, S., Tanaka, C., 2004. Manganese-enhanced magnetic resonance imaging (MEMRI) of brain activity and applications to early detection of brain ischemia. NMR Biomed. 17, 569–580.

Baratti, C., Barnett, A.S., Pierpaoli, C., 1999. Comparative MR imaging study of brain maturation in kittens with T1, T2, and the trace of the diffusion tensor. Radiology 210, 133–142.

Bilgen, M., Dancause, N., Al-Hafez, B., He, Y.Y., Malone, T.M., 2005. Manganese-enhanced MRI of rat spinal cord injury. Magn. Reson. Imaging 23, 829–832.

Derrick, M., Luo, N.L., Bregman, J.C., Jilling, T., Ji, X., Fisher, K., Gladson, C.L., Beardsley, D.J., Murdoch, G., Back, S.A., Tan, S., 2004. Preterm fetal hypoxia–ischemia causes hypertonia and motor deficits in the neonatal rabbit: a model for human cerebral palsy? J. Neurosci. 24, 24–34.

Farbman, A.I., Brunjes, P.C., Rentfro, L., Michas, J., Ritz, S., 1988. The effect of unilateral naris occlusion on cell dynamics in the developing rat olfactory epithelium. J. Neurosci. 8, 3290–3295.

Heckmann, J.G., Stossel, C., Lang, C.J., Neundorfer, B., Tomandl, B., Hummel, T., 2005. Taste disorders in acute stroke: a prospective observational study on taste disorders in 102 stroke patients. Stroke 36, 1690–1694.

Hwang, I.K., Kang, T.C., Lee, J.C., Park, S.K., An, S.J., Lee, I.S., Lee, Y.B., Sohn, H.S., Kang, J.H., Choi, S.Y., Won, M.H., 2003. Chronological alterations of calbindin D-28k immunoreactivity in the gerbil main olfactory bulb after ischemic insult. Brain Res. 971, 250–254.

Hwang, I.K., Lee, J.C., Cho, J.H., Yoo, K.Y., Kim, D.S., Nam, Y.S., Kim, W.K., Lee, I.S., Kang, T.C., Won, M.H., 2004. Very delayed neuronal loss occurs in the glomerular layer of the main olfactory bulb following transient ischemia in gerbils. Neurosci. Lett. 366, 272–276.

Margolis, F.L., . A marker protein for the olfactory chemoreceptor neuron. In: Bradshaw, R.A., Schneider, D. (Eds.), Proteins of the Nervous System. Raven, New York, pp. 59–84.

Nakashima, T., Kimmelman, C.P., Snow Jr., J.B., 1984. Histopathology of the olfactory pathway due to ischemia. Laryngoscope 94, 171–175.

Pautler, R.G., Koretsky, A.P., 2002. Tracing odor-induced activation in the olfactory bulbs of mice using manganese-enhanced magnetic resonance imaging. NeuroImage 16, 441–448.

Pautler, R.G., Silva, A.C., Koretsky, A.P., 1998. In vivo neuronal tract tracing using manganese-enhanced magnetic resonance imaging. Magn. Reson. Med. 40, 740–748.

Schaal, B., Hummel, T., Soussignan, R., 2004. Olfaction in the fetal and premature infant: functional status and clinical implications. Clin. Perinatol. 31, 261–285.

Schwob, J.E., 2002. Neural regeneration and the peripheral olfactory system. Anat. Rec. 269, 33–49.

Tan, S., Drobyshevsky, A., Jilling, T., Ji, X., Ullman, L.M., Englof, I., Derrick, M., 2005. Model of cerebral palsy in the perinatal rabbit. J. Child Neurol. 20, 972–979.

Van der Linden, A., Van Meir, V., Tindemans, I., Verhoye, M., Balthazart, J., 2004. Applications of manganese-enhanced magnetic resonance imaging (MEMRI) to image brain plasticity in song birds. NMR Biomed. 17, 602–612.

Van Heest, A.E., House, J., Putnam, M., 1993. Sensibility deficiencies in the hands of children with spastic hemiplegia. J. Hand Surg. [Am] 18, 278–281.

Winberg, J., Porter, R.H., 1998. Olfaction and human neonatal behaviour: clinical implications. Acta Paediatr. 87, 6–10.

Youngentob, S.L., Schwob, J.E., Sheehe, P.R., Youngentob, L.M., 1997. Odorant threshold following methyl bromide-induced lesions of the olfactory epithelium. Physiol. Behav. 62, 1241–1252.

Yu, X., Wadghiri, Y.Z., Sanes, D.H., Turnbull, D.H., 2005. In vivo auditory brain mapping in mice with Mn-enhanced MRI. Nat. Neurosci. 8, 961–968.